Spectrometer concept and design for X-ray astronomy using a blazed transmission grating

Kathryn Flanagan*[a], Minseung Ahn[a], John Davis[a], Ralf Heilmann[a], David Huenemoerder[a], Alan Levine[a], Herman Marshall[a], Gregory Prigozhin[a], Andrew Rasmussen[b], George Ricker[a], Mark Schattenburg[a], Norbert Schulz[a], Yong Zhao[a]
[a]MIT Kavli Institute for Astrophysics and Space Research, 77 Mass. Ave., Cambridge, MA 02139
[b]SLAC/Stanford University

ABSTRACT

We present a spectrometer design based on a novel nanofabricated blazed X-ray transmission grating which is modeled to have superior efficiency. Here we outline a full instrument design proposed for Constellation-X which is expected to give resolving powers ~2000 (HEW). The spectrometer advantages include lower mass budget and smaller diffractor area, as well as order-of-magnitude more relaxed alignment tolerances for crucial degrees of freedom than reflection grating schemes considered in the past[1,2,3]. The spectrometer readout is based on conventional CCD technology adapted to operate with very high speed and low power. This instrument will enable high resolution absorption and emission line spectroscopy in the critical band between 0.2 and 1.5 keV.

Keywords: grating, spectroscopy, X-ray, CCD, Constellation-X

1. INTRODUCTION

1.1 High resolution X-ray spectroscopy

The next generation of X-ray observatories will emphasize high spectral resolution and large effective area. Two current facility-class observatories, NASA's Chandra X-ray Observatory and ESA's XMM-Newton, both provide high spectral resolution in the soft X-ray band, employing grating spectrometers of sufficient resolution to isolate individual X-ray lines. This capability allows us to probe astrophysical processes in detail. Emission lines reveal temperature and density diagnostics, detailed velocity structure, ionization balance and elemental abundance; absorption spectroscopy probes accretion dynamics in AGN, and provides a powerful tool for studying the intergalactic medium. These are but representative examples of the power of high resolution spectroscopy in the soft X-ray band, and serve to illustrate why it is central to future planned missions. NASA's next X-ray Great Observatory, Constellation-X[4], is a spectral mission with high effective area whose hardware complement will include a grating spectrometer, a microcalorimeter, and a hard X-ray telescope. Pharos[5], a candidate Explorer mission, will exploit gratings to probe the WHIM, while vision missions such as Gen-X[6] will likely use gratings to push X-ray astrophysics into a new domain.

1.2 Candidate grating schemes

Two reflection grating schemes have been studied in considerable detail as excellent candidates for Constellation-X. The in-plane grating[2] (IPG), of which the RGS[7] on XMM-Newton is an example, exploits "grazing incidence" reflection to achieve a high projected line density, thereby providing high dispersion (and correspondingly high spectral resolution). Such an arrangement is limited by internal vignetting, and diffraction angles can be high, limiting the throughput. Refection gratings can also be used in an off-plane configuration. Compared with the IPG, the off-plane grating[3] (OPG) has intrinsically higher efficiency, but cannot exploit the line density in projection – its dispersion must come from the line density that is fabricated directly into the grating. This loss of spectral resolution is compensated by *subaperturing*: the superior grating efficiency implies that covering a subaperture of the optic will provide sufficient effective area, and subaperturing results in an effective narrowing of the mirror PSF for the spectrometer[8], thereby boosting the spectral resolution. Reorienting groups or modules of gratings results in further subdividing the PSF, allowing for even higher

* kaf@space.mit.edu; phone 617 258-7324; fax 617 253-8084

Optics for EUV, X-Ray, and Gamma-Ray Astronomy III, edited by Stephen L. O'Dell, Giovanni Pareschi
Proc. of SPIE Vol. 6688, 66880Y, (2007) · 0277-786X/07/$18 · doi: 10.1117/12.739941

spectral resolution[1,3,9]. To achieve optimal spectral performance, both of these reflection grating schemes must closely control their alignment and flatness.

X-ray transmission gratings have certain advantages over reflection grating schemes. They are extremely light, and require far less diffractor area since they are arranged normal to the incident beam. Because they do not rely on grazing-incidence reflection, flatness and alignment constraints are quite relaxed. For example, rotation of a grating by a small angle α around the normal to the plane of incidence will rotate reflected diffraction orders by ~2α for the IPG, while transmitted orders will be rotated by $\alpha(m\lambda/p)^2$, a reduction of several orders of magnitude for wavelength λ~1 nm, grating period p~100 nm, and m = diffraction order ~1-5. The OPG will be similarly impacted by its reflection geometry, although its alignment requirements differ from the IPG case[10]. All X-rays in the undispersed (zeroth) order pass through to the telescope focus, contributing to the throughput there. X-ray transmission gratings are insensitive to polarization at these wavelengths, and can be well modeled[11]. Like the OPG, transmission gratings must rely on the line density which is fabricated into the grating. A significant disadvantage of transmission gratings has been their inferior efficiency relative to reflection gratings. The Chandra High Energy Transmission Gratings[12] (HETG) are phase gratings, boosting the efficiency, but the light is dispersed symmetrically into plus and minus orders, necessitating a readout that captures both sets of orders.

1.3 Critical-Angle Transmission Grating (CAT) spectrometer

This paper introduces a new X-ray transmission grating spectrometer that captures the advantages of both reflection and transmission gratings. The spectrometer is based on a novel nanofabricated blazed X-ray transmission grating, the Critical-Angle Transmission (CAT) grating. The CAT grating is designed and modeled to have superior efficiency, comparable to off-plane reflection gratings, and like the OPG can be used in a subaperture arrangement to boost the spectral resolving power. It is a *blazed* grating, designed to cast virtually all of the dispersed light into a narrow angular range (rather than symmetric plus and minus orders), eliminating the need for a long readout detector. Relative to reflection gratings arrayed in analogous configuration, it has the advantages of lower mass, smaller diffractor area, significantly relaxed alignment tolerances, insensitivity to polarization, and does not deflect zeroth order (undispersed) photons away from the telescope focus. Details of the grating fabrication process, grating efficiency modeling and x-ray characterization are given elsewhere[13,14].

We present below a specific spectrometer implementation appropriate for Constellation-X, as a concrete illustration of instrument design and performance. The instrument combines an array of CAT gratings with a spectrometer readout based on conventional CCD technology adapted to operate with very high speed and low power. The gratings and CCDs build on successful instruments flown for Chandra and Suzaku. The spectrometer is estimated to deliver over 1000 cm^2 with resolving power $E/\Delta E$~2000(HEW) on Constellation-X, enabling critical science at soft energies. The grating and readout parameters can be optimized for the requirements of other missions such as Pharos, and the spectrometer is an excellent candidate for formation-flying arrangements.

2. GRATINGS

2.1 Critical angle concept

At the core of the instrument lies the CAT grating. It is not a phase grating like the Chandra HETG which exploits the phase-shifting properties of high-Z materials such as gold, but instead achieves high diffraction efficiency over a broad bandpass through reflection off the sidewalls of ultra-high aspect ratio (AR) grating bars[13]. These bars are inclined relative to the direction of the incident X-rays by an angle θ that is less than the critical angle for total external reflection $\theta_c(\lambda)$. Highly efficient sub-critical-angle reflection and grating diffraction conditions are fulfilled for a wide range of λ satisfying $\theta < \theta_c(\lambda)$. Incidence at these small angles leads to efficient blazing, and only orders on one side of the transmitted zeroth order beam need to be detected by the readout. Higher energy X-rays have a very shallow critical angle ($\theta_c(\lambda) < \theta$), and are mostly transmitted (apart from weak absorption by the grating bars) in zeroth order and are passed to the telescope focus where they are collected by the calorimeter (see Fig. 1).

Due to the small critical angles for $\lambda \approx$ 10-50 Å, high AR (~150) grating bars are required. Such high AR structures can be fabricated through the highly anisotropic KOH etching of crystalline silicon[15], resulting in atomically smooth

sidewalls defined by Si (111) lattice planes. To achieve high angular dispersion, the grating will have a period of only 100 nm. These considerations lead to the grating parameters outlined in Table 1.

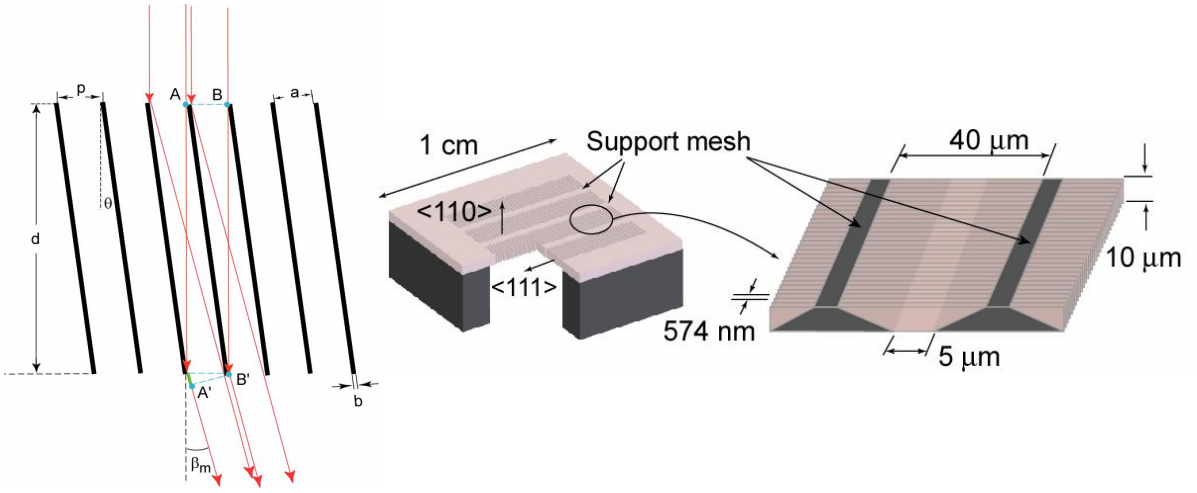

Figure 1. (left) Schematic of CAT grating principle. The CAT grating exploits the ultra-smooth sidewalls of silicon that can be fabricated using anisotropic etching. Efficient $2\pi m$ constructive interference from one grating line to the next is achieved by ensuring that the path length difference between A-A' and B-B' in the figure is given by $p\sin\beta_m=m\lambda$, where p is the grating period and m is the diffraction order. Efficient diffraction (i.e., blazing) is achieved when the diffracted order coincides with specular reflection off the grating sidewall, i.e., $\beta_m=2\theta$. High reflectivity is ensured when $\theta<\theta_C$, the critical angle for grazing-incidence x-ray reflection. (right) Schematic of a prototype CAT grating which has been fabricated on a silicon-on-insulator wafer.

2.2 Support structure

The diffracting elements are very thin and will require a hierarchy of support structures. A coarse support structure will be integrated with the 3.0 μm-thick grating. This support structure is not completely opaque to X-rays, and allows some photons to pass through, undiffracted and unabsorbed, to zeroth order. The structure is overlaid with a thick honeycomb, for a second level of support. The next level up is a 2-dimensional metal frame. The final grating facet size will be determined based on raytrace studies and fabrication constraints; the minimum size is 15 mm with a constant period, and the target is 100 mm size with the period varied across the grating to optimize resolving power. Larger structures will be matched to the optic modules through a grating integrating structure to eliminate further throughput losses. Grating parameters and support structure details are listed in Table 1 below.

Table 1. Grating parameters and support hierarchy for Constellation-X.

Grating Parameters
Period: 100 nm (10,000 lpmm)
Thickness: 3.0 μm
Graze angle: 1.5 degrees
Bar-to-period ratio: 0.2
Material: Si
Facet size: between 15 mm and 100 mm

Support Hierarchy
Coarse support (1D): integrated 3.0 μm thick with 0.1 μm line on 2 μm pitch
Thick honeycomb: 1 mm thick with 50 μm line on 1 mm pitch
Metal frame (2D): 2 mm thick with 2 mm line on 4 cm pitch

2.3 Prototype gratings

Prototype CAT gratings as shown below in Figure 2 have been developed by MIT's Space Nanotechnology Laboratory. The results of these efforts are reported elsewhere[13,14]. The prototypes represent small x-ray tested silicon gratings which have met milestones of aspect ratio >150, duty cycle (bar-to-period ratio) <0.15, microroughness 0.2 nm, and thickness of 10 microns. Preliminary efficiency measurements on a CAT grating show good agreement with the model. Future development efforts will address grating period, facet size, and structural support.

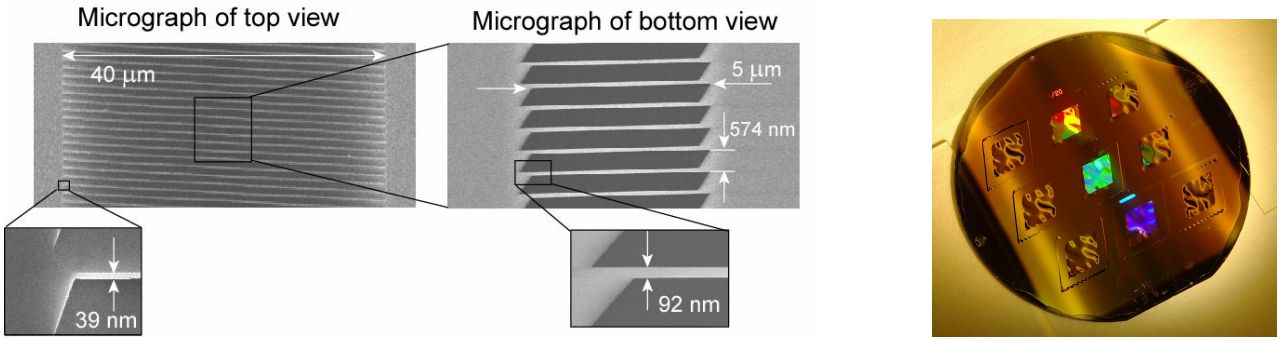

Figure 2. Prototype CAT grating developed by the Space Nanotechnology Laboratory at MIT. These prototypes have a pitch of 574 nm. The roughness of the (111) sidewalls was measured by AFM to be 0.2 nm, which is expected to have negligible impact on reflectivity. (left) Electron micrographs of top and bottom views of the CAT prototype. The insets show some individual grating lines which are 39 nm wide at the top and 92 nm wide at the bottom. (right) A photograph of six CAT gratings at an intermediate fabrication step are shown on a 100 mm-diameter Si substrate.

2.4 Efficiency modeling

Efficiency modeling of proposed Constellation-X gratings was performed using the GSOLVER[16] software, which is based on a hybrid rigorous coupled wave and modal analysis. Details of the modeling approach and efficiency testing of prototypes are reported elsewhere[14]. Similar approaches have been used previously to model related existing zone plate structures[17]. We find that silicon alone, without a metal coating, will provide high efficiency. This eliminates the risk of diminished high order efficiency due to deposition of a rougher metal overlayer. Our simulations also predict that CAT gratings are highly insensitive to polarization (<0.25% relative difference in efficiency between TE and TM modes at Constellation-X wavelengths). The grating parameters appropriate for a Constellation-X spectrometer, shown in Table 1, were used to model the efficiencies in this paper. The results are shown in Figure 3 below.

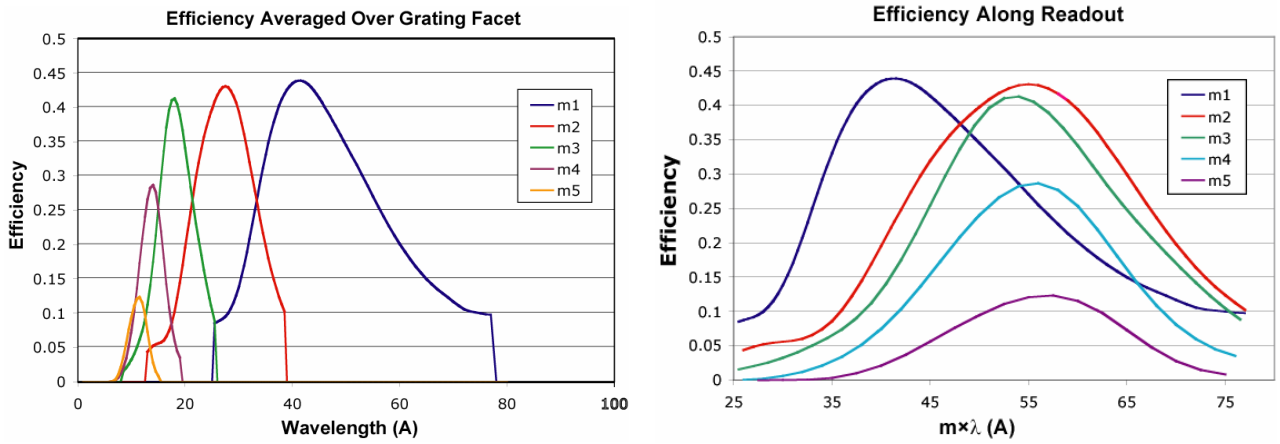

(a) (b)

Figure 3. (a) Grating efficiency for orders 1-5 falling on the readout. Efficiencies were modeled with GSOLVER. We included a range of incidence angles expected for a grating facet of ~10 cm for realism. (b) Plot of grating efficiency as a function of mλ (which corresponds to position along the readout) shows that most of the efficiency is captured by CCDs spanning the range 25.5 Å < mλ <77 Å.

The CAT grating as optimized for Constellation-X is modeled to have very high efficiency (~40%) in the first three orders. Recall that the dispersion angle θ is related to order m, wavelength λ and period p by the grating equation (for

normal incidence) $m\lambda = p \sin\theta$. The plot in Figure 3b therefore shows that the grating distributes the dispersed X-rays with high efficiency over a relatively small angular range. This *blaze* property means that a short readout covering 25.5 Å < mλ < 77 Å will capture most of the dispersed photons. Moreover, the readout is located at sufficiently large dispersion that the spectrum will be captured at high spectral resolution. Since multiple orders are spatially overlapped, X-ray CCDs with moderate spectral resolution are used to provide order sorting.

3. CCD READOUT

The focal plane readout proposed for use with Constellation-X consists of back-illuminated (BI) X-ray CCDs fabricated at MIT Lincoln Laboratory (MIT/LL). The CCDs are based on enhanced, multi-output structures similar to those used in previous flight programs. The backside treatment utilizes the molecular beam epitaxy (MBE) process recently developed at MIT/LL. The low energy X-ray performance of MBE BI CCDs is similar to the performance of BI CCDs flown on Suzaku and is by far superior to that of any other known BI CCD technology, both in terms of energy resolution as well as quantum efficiency. As shown in Figure 4, each CCD device in the array will have dual parallel sections, each 1600 columns by 512 rows. The dimensions of the resulting imaging array will be 24.0 mm [dispersion direction] x 15.36 mm [cross dispersion direction]. The image array pixels will be 15 microns x 15 microns, while the frame store pixels will be 7.7 microns by 15 microns. In order to allow high readout speed and low dark current (thus enabling near room temperature operation), each CCD will be partitioned into 16 blocks, each with its own output. To increase readout speed even further we can utilize on-chip pixel summation, which will also provide optimum sampling of the line spread function (LSF). We estimate that a 2 column x 8 row summed "superpixel" with dimensions of 30 microns x 120 microns will be optimal. Summed in this way, the CCD frame rate will be 72 Hz (13.8 ms frame time). The effective "superpixel" size (and the frame rate) can be modified as needed in software to optimize a given observation.

The gaps between the CCDs will be 0.4 mm, the same as achieved for ACIS-S on Chandra, and about 20 devices will be needed for each readout (see Section 4.2). The analog signal processing circuits and digital converters will be edge-mounted as hybrid circuits adjacent to the CCD, allowing for a very fast and low power readout. We estimate that each 20 chip long readout will require only 15 W of power. An optical blocking filter consisting of 100 Å of Al will be deposited directly on the surface of the CCDs.

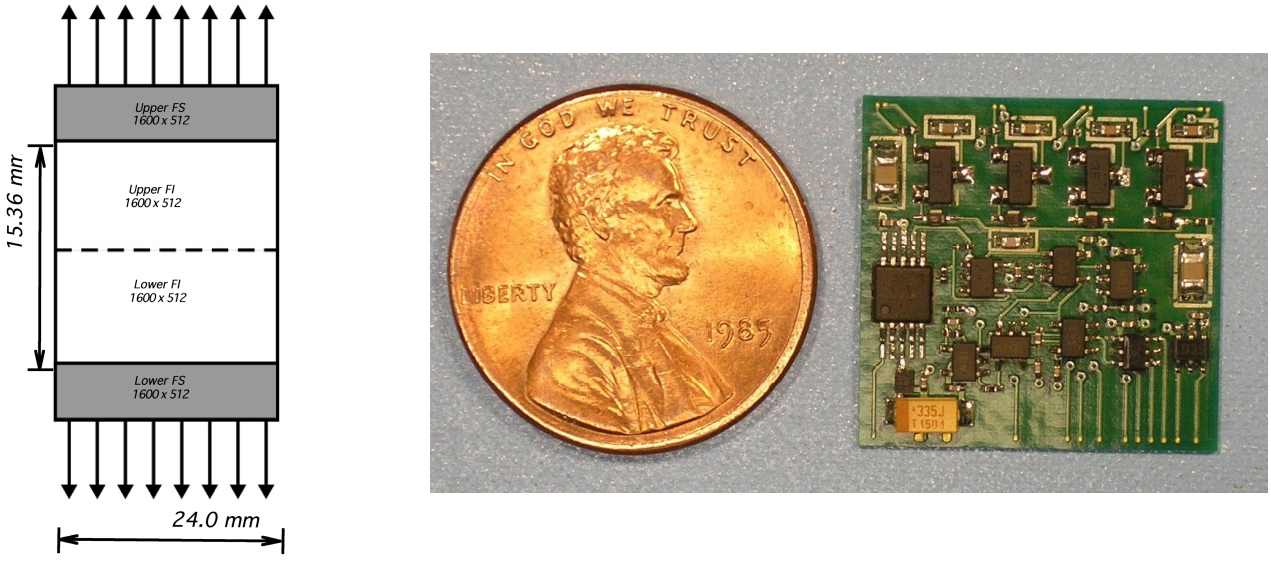

Figure 4. (left) Each CCD device will have dual parallel sections, 1600 columns by 512 rows, and be partitioned into 16 blocks, each with its own output. Image array pixels will be 15 μm x 15 μm summed into larger "superpixels." (right) A compact low power hybrid circuit for fast CCD readout was developed and successfully tested.

4. INSTRUMENT DESIGN AND LAYOUT

4.1 Overall concept

The transmission grating spectrometer is arranged in a Rowland circle geometry, much like the Chandra High Energy Transmission Grating Spectrometer (HETGS). This is illustrated in Figure 5. It will include grating facets arrayed "downstream" of the Constellation-X optic, intercepting sectors of the converging beam. Since the gratings are blazed, the CCD readout will capture only one set of orders, and only over a limited range of wavelengths where the grating efficiency is high. The "zeroth order camera," which captures the undispersed beam, is the calorimeter itself: zeroth order photons will enhance the overall throughput to the calorimeter.

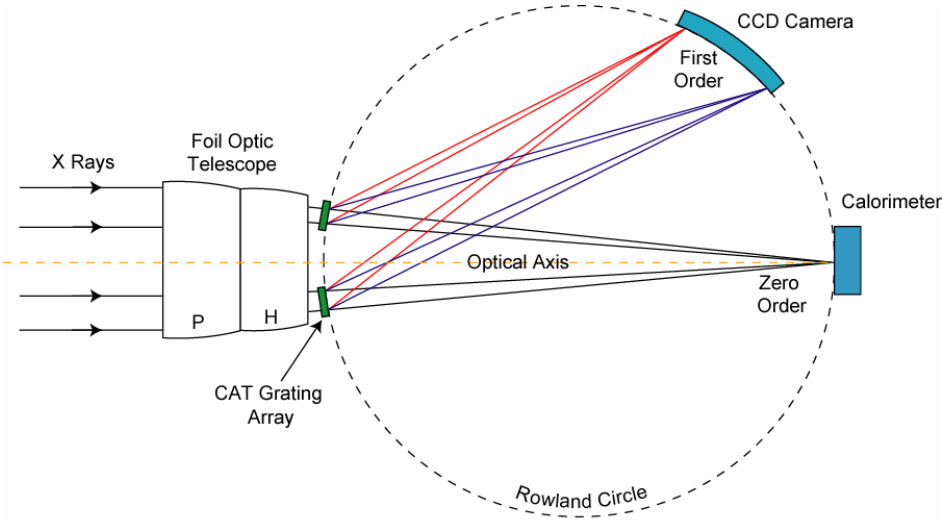

Figure 5. The transmission grating spectrometer follows a Rowland circle geometry. The calorimeter lies at the zero-order focus. The CCD readout captures multiple overlapping orders and uses its moderate spectral resolution to distinguish among them.

The high-efficiency blazed gratings will be fabricated at MIT's Space Nanotechnology Laboratory, exploiting the crystal planes of silicon[18] to provide super-smooth, precisely shaped and aligned grating bars of very high line density (10,000 lines per mm or 100 nm period). The gratings will be arranged on a *subaperture* of the optic, narrowing the effective LSF and significantly boosting spectral resolution. The ability to custom "tailor" the grating period with the MIT Nanoruler[19,20] will allow improved spectral resolving power, mitigating or eliminating traditional negative impacts such as the finite size of grating facets. The Rowland geometry will likewise be optimized to take advantage of the blazed nature of the grating array.

The spectrometer design overlaps multiple diffracted orders with high efficiency in the same region of the readout. The X-ray CCD provides the spectral resolution to sort and distinguish these orders. The CCDs will be based on conventional devices, but with low power, low mass and high readout speed. This high readout speed is matched to the large mirror area of Constellation-X and allows stray light background rejection to be achieved with a much thinner optical blocking filter. The end result is very high CCD efficiency and high spectrometer throughput.

4.2 Instrument layout

The spectrometer configuration described below used as its basis the reference information[21] package provided for the Science Enhancement Package RFI for Constellation-X. We restrict the discussion to the basic configuration consisting of four Soft X-Ray Telescopes (SXT) on an Atlas V. For the grating spectrometer, each grating array will cover four out of the ten azimuthal sectors of an SXT optic, as illustrated by the "shadowgram" of Figure 6. Gratings will cover the "downstream" side of two adjacent mirror sectors, or an angle of ~72 degrees; they will also cover two symmetrically

placed mirror sectors on the opposite side of the optic. This arrangement constitutes a single grating array and provides an appropriate subaperture to give a narrow LSF. The gratings will be arrayed only along the *outer* annulus, down to the "gap" in the mirror between inner and outer shells. Mirror shells inward of the gap are left open to preserve high-energy throughput to the calorimeter. This arrangement allows some of the grating support structure to be "hidden" behind SXT supports and in the unoccupied gap.

The instrument for Constellation-X incorporates two independent subapertured grating arrays, each with its own readout, as shown in Figure 6. Both of these grating arrays are arranged on a single SXT, leaving the remaining SXTs untouched. This configuration allows use of a single integrating structure, saving mass. With this arrangement, effective area requirements are met as shown in Section 5.1, and the data from all instruments on Constellation-X are captured simultaneously. However, other spectrometer implementations (e.g., insertable/retractable grating wheels as on Chandra) could also be considered.

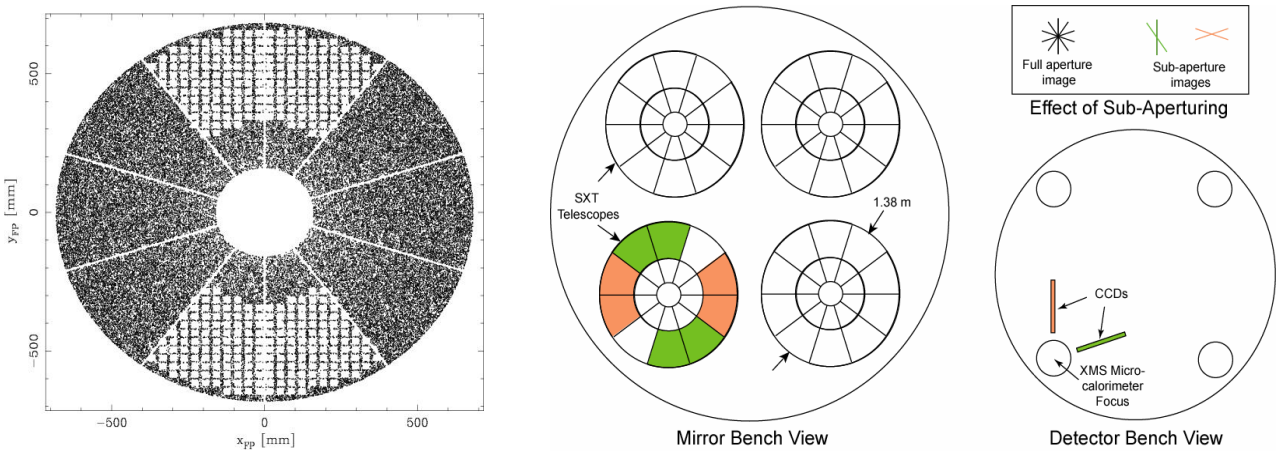

Figure 6. A basic grating array covers about 40% of an SXT mirror, in two symmetrically opposing sectors. This is illustrated by the "shadowgram" at left, showing gratings arrayed behind 4 of the 10 mirror sectors of one of the SXT telescopes. Only the outer annulus of the optic is covered by gratings. The instrument configuration has two independent grating arrays on a single SXT, as illustrated in the center figure above. Each array has its own readout, as shown in the figure at right, representing a top view of the focal plane. At the focus of each SXT is a calorimeter. As shown, the gratings are placed on only one of the four SXTs, and share the same calorimeter as the zero order camera.

The CCDs and gratings are arranged along a Rowland torus (a three-dimensional analogue to the Rowland circle in Figure 5). The details of the arrangement depend on the scheme used to optimize the resolving power. Since the gratings are blazed, the CCDs need capture only a limited region of the dispersed spectrum (corresponding to 25.5 Å<mλ<77 Å as seen in Figure 3(b), or dispersion angle $1.46° < \theta < 4.42°$). The grating line density and Rowland diameter then define the length and placement of the readout. We estimate that each readout will require about 20 CCD devices given grating placement relative to the 10 m focal length of Constellation-X. The placement of the readout electronics assemblies is not critical, provided they are located within ~1 m of the devices. (They may even be placed *under* the readout for compact arrangement.) Details of the instrument layout and accommodations are given in Table 2.

Table 2. Engineering and accommodations details of spectrometer.

Cost, Mass and Power
Grating Mass: 23 kg
CCD Readout Mass: 2x19 kg
Total Mass: 61 kg
Total Power: 30 W

Accommodations
Total grating coverage: 288° on one SXT from r = 324 to 659 mm (shells 32-128)
Grating envelope: < 80 mm
Rowland diameter: 9250 mm
Readout range: mλ = 25Å to 77Å; 231 mm to 719 mm from calorimeter
Readout envelope: < 65 mm
Readout length: 488 mm or 20 CCD devices (each readout)
Dispersion range: 1.46 to 4.42 degrees
Size of electronics boxes: 60 cm x 15 cm x 15 cm (detector)
30 cm x 30 cm x 20 cm (Detector Electronics Assembly)
30 cm x 30 cm x 30 cm (Data Processing Assembly, Power Supply and Mechanism Controller)
Placement of electronics boxes: PSMC and DPA within 2 meters, and DEA within ~1 m of detector assembly

5. INSTRUMENT PERFORMANCE

Spectral resolving power and effective area are the two primary figures of merit which define the science return of the instrument. The useful wavelength range will also contribute to the instrument capability. Below we present performance estimates based on the parameters and configurations discussed previously. However, it should be noted that latitude exists to fine-tune the instrument capabilities (e.g., adjust the effective area, wavelength coverage and spectral resolving power.)

5.1 Effective area

In order to calculate effective area, we considered structural blockage, grating efficiency, CCD efficiency and optical blocking filter transmission. We assumed the mirror input model for the 4SXT configuration provided in the RFI. As shown at the left in Figure 7, the transmission grating spectrometer (TGS) provides 1000 cm^2 of effective area at energies above ~320 eV, and extends the wavelength coverage as far down as ~165 eV with somewhat less effective area. All of this area represents high spectral resolving power, but it represents a "tradeoff" as shown in the right of the figure. Mission effective areas (i.e., grating plus calorimeter), with and without the grating spectrometer, are given in the right of Figure 7. The introduction of the grating spectrometer, with its support structures, will block some of the light going to the calorimeter. Nevertheless, it allows the 6 keV system effective area requirement to be met with margin, and the 1.25 keV requirement to be met as well (but without margin). The impact at high energies (e.g., 6 keV and above) is relatively benign because the gratings are effectively "transparent" at high energies and, except for structural blockage, the X-rays are primarily transmitted in the zeroth order.

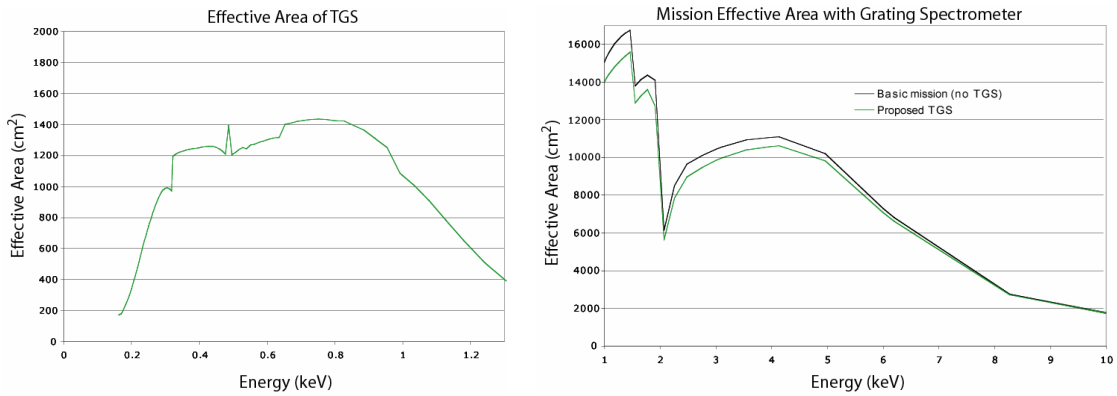

Figure 7. (left) The grating spectrometer provides 1000 cm^2 or more of system area at energies above ~320 eV (wavelengths shorter than 38.5 Å). The instrument energy range goes down to ~165 eV, but with lower effective area. (right) The grating spectrometer reduces the system effective area slightly at energies above 1 keV, but mission requirements are met.

5.2 Spectral resolving power

As a starting point to assess resolving power, we adapted the Chandra HETG error budget equations[12] to the grating spectrometer proposed for Constellation-X. We identified the terms expected to have significant impact (optic PSF, grating size, observatory level effects) and obtained a preliminary estimate of spectral resolution. Under current fabrication practice, period variations are not expected to significantly impact the spectral resolution. Readout time and CCD pixel size are also insignificant contributors. As noted previously, crucial alignment and mounting tolerances are much looser than for reflection grating schemes, so that gravity sag, thermal distortions, etc., are lesser considerations.

The most significant factor in correctly assessing the spectral resolution is the optic. This is even less straightforward under subaperturing. We carried out two separate raytraces of the instrument. For both raytraces, we assumed a 12.5 arcsec HPD mirror with slope errors to model the optics, and 4.1 arcsec (2-dimensional HPD) alignment errors to model Gaussian telescope-level effects. (The breakdown of assumed contributors is given in Table 3.)

Table 3. Assumed breakdown of contributions to "nominal" Con-X optic PSF.

Assumed Optic Errors (arcsecs HPD)
SXT on-orbit performance: 12.48"
Telscope level effects: 4.1" comprised of:
Attitude / knowledge drift: 2"
SXT / SI focal plane drift (thermal): 2"
Telescope mounting strain: 2"
SXT / SI vibration effects: 2"
SXT / SI misalignment (off-axis error): 1"
SXT / SI focus error: 0.2"

In the first raytrace, we assumed 15 mm grating facets with uniform period, arrayed with a symmetry axis through the zeroth order. (In practice, we expect to use much larger facets and chirp or vary the period to compensate. Arraying with a symmetry axis through the blaze may improve the resolving power.) In the second raytrace, a Wolter II optic was modeled without mirror scatter. The gratings were 100 mm facets arranged on an off-center Rowland circle to optimize the spot size at blaze. Based on the bounds provided by these two raytraces, we have provisionally accepted that the resolving power is approximated by R(HEW) ~ 44mλ (Å) or R(FWHM) ~ 29mλ (Å). Figure 8 incorporates this result. The resolving power is "provisional" because we do not have a mirror model that we can be confident accurately represents the flight optics. Critical to the resolving power estimate is the assumption that slope errors, not alignment errors, dominate the optic PSF. If this is not true, it will negatively impact any grating arrangement employing subaperturing[21]. In addition, the telescope-level effects must be controlled, although the limits we have assumed in Table 3 are not unduly restricting.

A significant contributor to high spectral resolution is the fact that the instrument brings in shorter wavelengths at higher orders, increasing the resolving power there. The order-by-order resolving power is shown at the left in Figure 8. Since a given wavelength is captured in multiple orders, an efficiency-weighted resolving power is a useful figure of merit. This is shown at the right in Figure 8. The calculated HEW resolving power exceeds 2000 for a nominal Constellation-X optic as parameterized in Tables 1 and 3. If the final optic meets the goal of 5 arcsecond, then the spectrometer performance is much improved, expected to exceed 5000 (HEW).

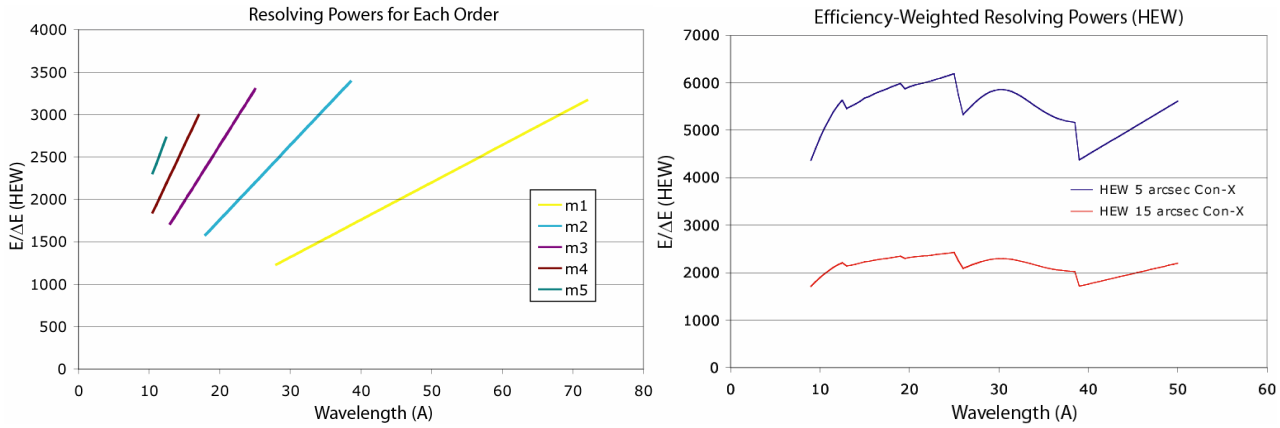

Figure 8. (left) Resolving power (HEW) for each order where grating efficiency is greater than ~10%. A given wavelength can be captured on the readout in several orders (each order with a different resolving power), so an efficiency-weighted resolving power, shown at right, is an appropriate figure of merit. These results comes from two different raytraces and have an error of ~25%. The figure at right shows estimated spectrometer performance R(HEW) >2000 for a "nominal" optic PSF (as outlined in Table 3) and R(HEW)>5000 for a "goal" PSF on Constellation-X. The HEW figure of merit is about 1.5 times higher than the FWHM equivalent, so that R(FWHM)>1300 for the "nominal" optic, and R(FWHM)>3000 for the "goal" optic.

The fact that the zeroth order photons are detected by the XMS (with larger pixel size than the CCD) deserves mention. The zeroth order will not impact the spectral resolution itself, but can impact the absolute wavelength scale. For our baseline configuration using a Lorentzian form for the grating LSF, we estimate that a line sampled with 4 bins per FWHM and 10 counts peak can be centroided to 0.1×FWHM (and less in proportion to 1/sqrt(max counts)), a desirable target for the dispersed line centroid. The calorimeter sampling is less (~3 pixels per resolution element), but is adequate for counting statistics to dominate the centroid error. Thus, any grating observation will easily have sufficient counts to centroid the zeroth order to the same level as the line, yielding a wavelength accuracy on the order of 0.2×grating FWHM. However, to maintain an absolute wavelength scale in order to conduct accurate velocity measurements, there needs to be length reference between the calorimeter and the readout with a precision of better than about 0.1×grating FWHM. We are aware of at least one implementation at reasonable cost.

6. SCIENCE ENABLED BY THE INSTRUMENT

High resolution spectroscopy below ~1.5 keV is essential for full Constellation-X science return. Within this range lies a rich array of X-ray lines, including L-shell lines of Fe and K-shell lines of He-like and H-like ions from N to Si. These lines provide temperature, density and ionization diagnostics, and sensitively probe velocity structure. In absorption, we find a powerful tool to detect and characterize baryonic matter "hidden" in the intergalactic medium, and to study highly ionized outflows seen in absorption against the background of their bright AGN. The powerful science enabled by this grating spectrometer is more fully elucidated elsewhere[4] and will not be presented in full. Instead, we present in Figure 9 two simulations to illustrate the science capability of the CAT grating spectrometer. An example of a warm absorber (left) shows absorption features in the spectrum. The spectrometer is expected to be sensitive to much lower columns, and will allow measurement of absorption features out to redshift z=2. Thus, the spectrometer will address the WHIM, a

key science area of Constellation-X. At right is an emission line spectrum of Capella in the Ne IX region, focusing on density-sensitive He-like lines. Emission lines provide critical diagnostics of the emitting plasma.

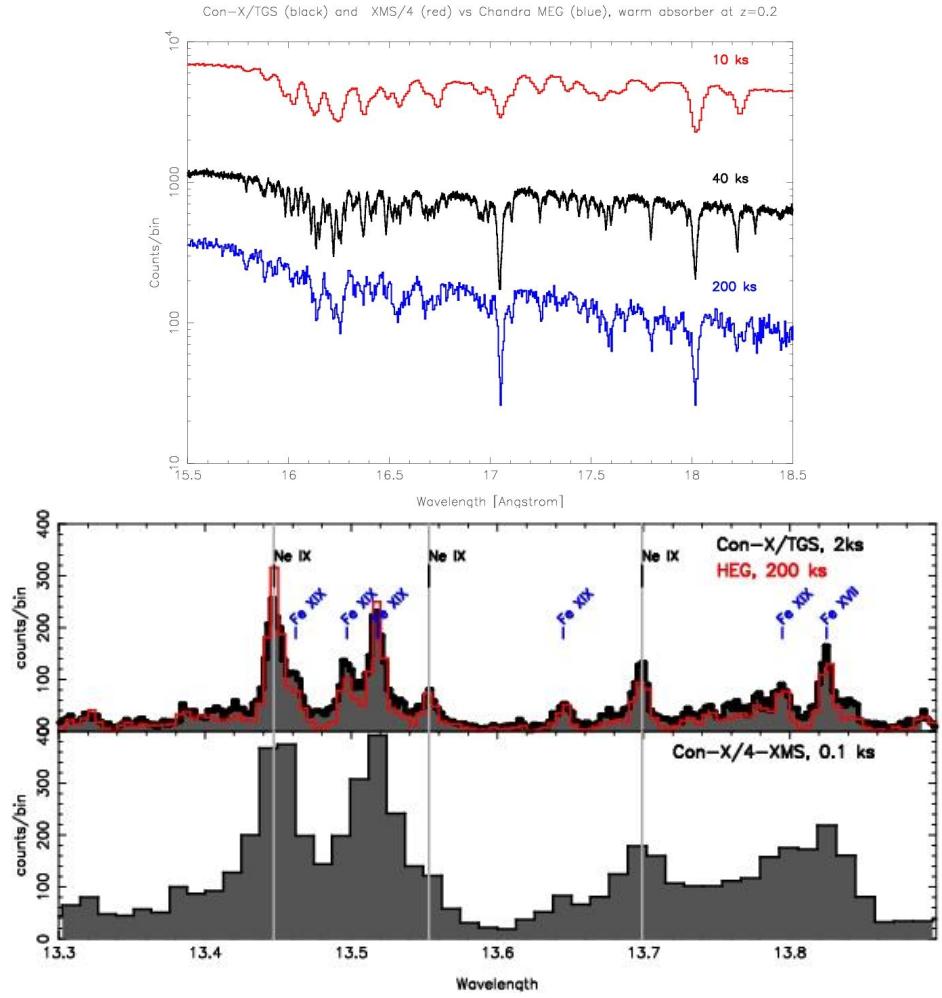

Figure 9. (top) The spectrum at the top shows a simulation of a warm (10^5K) absorber at z=0.20 (Fe XVII/XVIII line region). The top curve illustrates a spectrum from the calorimeter, the middle curve from the CAT spectrometer in 40 ks, and the bottom curve from Chandra in 200 ks. The CAT spectrometer has a bandwidth up to 77 Å with R ~ 2000 allowing absorption line detection and diagnostics well beyond z = 1. With increased exposure, the spectrometer will be sensitive to columns as much as two orders of magnitude lower, enabling detection of the WHIM. This is a significant science goal of Constellation-X, and the prime science of the candidate Explorer Pharos. (bottom) Simulation of Capella, a bright, coronally active binary, emphasizing the Ne IX region of density-sensitive He-like lines. A 2 ks observation with the CAT grating modeled for Con-X (labeled "TGS") is comparable to a 200 ks spectrum with the Chandra HEG grating. A calorimeter spectrum (below, right) cannot capture the details. Emission line spectroscopy enabled by the instrument includes stellar coronae, disks, winds and accretion.

ACKNOWLEDGMENTS

Support for this work was provided by NASA through ROSES Grants NNG05WC13G and NNX07AG98G (for the gratings) and NNG05WC03G (for the CCDs). We acknowledge further NASA support through the Smithsonian Astrophysical Observatory contract SV3-73016 to MIT. NASA also provided support for CCD development through Constellation-X grant NAG5-12377. We gratefully acknowledge a Samsung fellowship, and support by Kavli Institute internal funds. We acknowledge support by MIT Lincoln Laboratory for development of the hybrid amplifier.

REFERENCES

[1] Flanagan *et al.*, "The Constellation-X RGS options: raytrace modeling of the off-plane gratings", in *UV and Gamma-Ray Space Telescope Systems*, G. Hasinger and M.J.L.Turner, eds., Proc. SPIE **5488**, 515-529 (2004).

[2] Kahn, S.M., Paerels, F.B., Peterson, J.R., Rasmussen, A.P., Schattenburg, M.L., Ricker, G.R., Bautz, M.W., Doty, J.P., Progozhin, G.Y., Nousek, J.A., Burrows, D.N., Hill, J.E., and Cash, W.C., "Large-area reflection grating spectrometer for the Constellation-X mission", in *EUV, X-Ray and Gamma-Ray Instrumentation for Astronomy X*, O.H. Siegmund and K.A. Flanagan eds., Proc. SPIE **3765**, 94-103 (1999).

[3] Cash, W.C., "X-ray optics. II - A technique for high resolution spectroscopy", Appl. Opt. **30**, 1749-1759 (1991).

[4] http://constellation.gsfc.nasa.gov/documents/science/science_goals/sci_goals_booklet_0505.pdf

[5] Elvis, M., Nicastro, F., Fiore, F., Phillips, L.A., Murray, S.S., Flanagan K.A. and Ramsey, B.D., "Pharos: GRB/WHIM science to mission design flowdown", in *UV, X-Ray, and Gamma-Ray Space Instrumentation for Astronomy XV,* O.H.W. Siegmund ed., Proc. SPIE **6686**, in press (2007)**.**

[6] Brissenden, R., Cameron R., Fabbiano G., White, N., Zhang, W., "The Generation-X X-ray Observatory Vision Mission and Technology Study", AIAA-2004-6041, 2004.

[7] Den Herder, J.W. *et al.,* "The Reflection Grating Spectrometer on board XMM-Newton," Astron. and Astrophys. **365**, L7-L17 (2001)**.**

[8] Cash, W., "X-ray optics: a technique for high resolution imaging", Appl. Opt., **26**, 2915-2920 (1987).

[9] McEntaffer, R.L., Cash, W.C. and Shipley, A.F., "Off-plane gratings for Constellation-X", in *X-Ray and Gamma-Ray Telescopes and Instruments for Astronomy*, J.E. Truemper and H.D. Tananbaum, eds., Proc. SPIE **4851**, 549-556 (2003).

[10] Cash, W.C., and Shipley, A.F., "Off-plane grating mount tolerances for Constellation-X," in UV and Gamma-Ray Space Telescope Systems, Guenther Hasinger and Martin J. L. Turner, eds., Proc. SPIE **5488**,335-340 (2004).

[11] Flanagan, K.A., Markert, T.H., Davis, J.E., Schattenburg, M.L., Blake, R.L., Scholze, F., Bulicke, P., Fliegauf, R., Kraft, S., Ulm, G. and Gullikson, E.M., "Modeling the Chandra high-energy transmission gratings below 2 keV", in *X-Ray and Gamma-Ray Instrumentation for Astronomy XI*, K.A. Flanagan and O.H. Siegmund eds., Proc. SPIE **4140**, 559-572 (2000).

[12] Canizares, C.R., Davis, J.E., Dewey, D., Flanagan, K.A., Galton, E.B., Huenemoerder, D.P., Ishibashi, K., Markert, T.H., Marshall, H.L., McGuirk, M., Schattenburg, M.L., Shulz, N.S., Smith, H.I., Wise, M., "The Chandra High-Energy Transmission Grating: Design, Fabrication, Ground Calibration, and 5 Years in Flight", PASP **117**, No. 836, 1144-1171 (2005).

[13] Ahn, M., Heilmann, R.K., and Schattenburg, M.L., "Fabrication of ultra-high aspect ratio freestanding gratings on silicon-on-insulator wafers," J. Vacuum Science and Technol., Nov/Dec 2007 (*in press*).

[14] Heilmann, R.K., Ahn, M., Gullikson, E.M, and Schattenburg, M.L., *in preparation*.

[15] Hölke, A. and Henderson, T.H., "Ultra-deep anisotropic etching of (110) silicon", J. Micromech. Microeng. **9**, 51 (1999).

[16] http://www.gsolver.com/

[17] Hambach, D., Schneider, G., and Gullikson, E.M., "Efficient high-order diffraction of extreme-ultraviolet light and soft x-rays by nanostructured volume gratings", Opt. Lett. **26**, 1200 (2001).

[18] Franke, A.E., Schattenburg, M.L., Gullikson, E.M., Cottam, J., Kahn, S.M. and Rasmussen, A., "Super-smooth x-ray reflection grating fabrication", *J. Vac. Sci. Technol. B* **15**, 2940-2945 (1997).

[19] Chen, C.G., Konkola, P.T., Heilmann, R.K., Joo, C. and Schattenburg, M.L., "Nanometer-accurate grating fabrication with scanning beam interference lithography," *Proc. SPIE* **4936***, Nano- and Microtechnology: Materials, Processes, Packaging, and Systems* (SPIE, Bellingham, WA), ed. D.K. Sood, 126-134 (2003).

[20] Konkola, P., Chen, C., Heilmann, R.K., Joo, C., Montoya, J., Chang, C.-H. and Schattenburg, M.L., "Nanometer-level repeatable metrology using the Nanoruler," *J. Vac. Sci. Technol. B* **21**, 3097-3101 (2003).

[21] https://conxproj.gsfc.nasa.gov/business/Con-X_RFI.htm

[22] Rasmussen, A., Aquila, A., Bookbinder, J., Chang, C.-H., Gullikson, E., Heilmann, R.K., Kahn, S.M., Paerels, F. and Schattenburg, M.L., "Grating arrays for high-throughput soft x-ray spectrometers", in *Optics for EUV, X-Ray and Gamma-Ray Astronomy,* O.Citterio and S.L. O'Dell eds., Proc. SPIE **5168**, 248-259 (2004)**.**